Synthesis of Nanosized Titanium Oxide and Nitride Through Vacuum Arc Plasma Expansion Technique

A.A. Lepeshev, I.V. Karpov, A.V. Ushakov, L.Yu. Fedorov, A.A. Shaihadinov
Siberian Federal University, Krasnoyarsk,660041, Russian Federation
sfu-unesco@mail.ru

Abstract. Physical vapor deposition techniques such vacuum arc plasma deposition – which are very commonly used in thin film technology – appear to hold much promise for the synthesis of nanocrystalline thin films as well as nanoparticles. Monodisperse and spherical titanium oxide and nitride nanoparticles were produced at room temperature as a cluster beam in the gas phase using a cluster-deposition source. Using the basic principles of the gas condensation method, this study has developed vacuum arc nanoparticle synthesis system. We demonstrate that major process deposition parameter is the pressure in the plasma chamber. This is the major advantage of these techniques over thermal evaporation. Our method affords TiN powders with high specific surface areas exceeding 200 m^2 g^{-1}. TEM micrograph of TiO_2 nanoparticles prepared at an oxygen pressure of 60 Pa show an average particle size of 6 nm. TiO_2 nanoparticles prepared at an oxygen pressure of 70 Pa were observed to have not a reduced average particle size.

Keywords: nanoparticles, vacuum arc, TEM micrograph, X-ray analysis.

In recent years, research involving nanophase materials has shown an unprecedented growth because such materials possess unique properties that are often superior to those of conventional large-grained polycrystalline materials. For example, research into applications for titanium nitride nanocrystals include use in coatings and microcoatings in hard thin films, and to improve hardness in alloys, ceramics and for use in automotive, aerospace and industrial sectors, to improve reaction kinetics, as a binder in nanolayers, and in other coatings, plastics, and polymers [1, 2]. Further application could arise in sensor technology, optoelectronics and for space structures. TiO_2 nanoparticles has been intensively studied due to its interesting properties. Indeed, TiO_2 is, for instance, promising for the development of powerful anti-bacterial and self-cleaning coatings, or for building efficient solar cells [3]. Recently, nanocomposites in which oxide nanoparticles having high dielectric constant dispersed in an organic matrix with high breakdown field have emerged as attractive candidates for large electrical energy storage [4-6], which is required for mobile electronic devices, hybrid electric vehicles, and stationary power systems[7-9]. While batteries are used almost exclusively in these applications, high energy-density capacitors are showing great promise [7, 8]. Its high refractive index also allows its use in the development of optical waveguides, antireflection and multilayer optical coatings [10]. Many research groups are therefore working on the TiO_2 doping as well as on ways to improve its crystallinity. TiO_2 nanoparticles may be an alternative approach to solve the aforementioned problems. They offer interesting advantages over thin films such as increased active surface area and reduced electron-hole pair recombination.

Nanoparticles can be synthesized by many techniques, including sol-gel process, hydrothermal methods, sparking process, laser ablation, laser pyrolysis, spray deposition, MOCVD and RF induction plasma [11-13]. The chemical methods of preparation suffer from an important drawback: the use of organic precursors or solvents. Indeed, these may lead to some unwanted impurities and are not environment-friendly which limits the development of efficient devices and the potential industrial applications, respectively. The physical production techniques (laser ablation and RF induction plasma),

although environment-friendly, are limited by the size of the produced samples which is not sufficient for a large-scale production. We recently showed the possibility of synthesizing TiN nanoparticles by a more suitable physical method of preparation: vacuum arc sputtering. This is a very interesting technique for industries for many reasons: metal targets are used, the stoichiometry is controllable, the environment is respected and a large-scale production is possible [14]. Using the basic principles of the gas condensation method, this study has developed vacuum arc nanoparticle synthesis system. We demonstrate that major process deposition parameter is the pressure in the plasma chamber. This is the major advantage of these techniques over thermal evaporation.

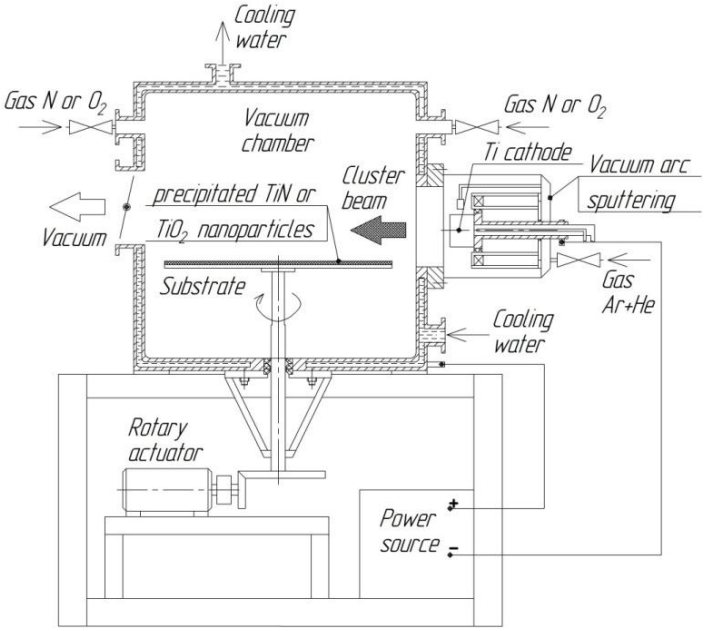

Fig. 1. A schematic diagram of the cluster-deposition apparatus used for the growth of TiO_2, TiN.

Plasma-condensation-type cluster-deposition systems have been used to produce highly monodisperse metal and alloy nanoparticles of sizes varying from a few tens to several thousands of atoms using an inert gas condensation principle. A schematic diagram of the basic experimental system for sputtering of nanoparticles is shown in Fig. 1. A 400 mm long axial vacuum arc sputtering source suitable for 80 mm diameter targets was used. This source can operate at the maximum input power level of 40 kW (dc). The sputter source was fed by a series dc power supply (80 V±300mV, 40–500 A ±1 A). The series vacuum chamber (600 mm diameter and 600 mm tall) with 4 ports was initially evacuated to10^{-3} Pa by an oil-vapor vacuum pump. A highly pure inert gas (He, Ar were all used) at a constant, pre-selected pressure – typically between 5 and 100 Pa – was then allowed into the chamber, and sputtering was carried out in flowing gas. The substrate was held at a distance of 200 mm from the sputtering target. The stainless steel types of substrates were successfully used. Both horizontal as well as vertical (bottom upwards) sputtering geometries can be used to deposit nanoparticles. However, during the deposition of nanoparticles, it was found preferable to use a horizontal geometry. The ambient pressure was typically maintained at values higher than those required in thin film processing to ensure substantial collision between the sputtered atoms and the inert gas atoms. This leads to cluster formation and reduces the mean energy with which these clusters approach the substrate. On the other hand, the substrate was held at temperatures much lower than in thin film formation (typically 300 K).

This tends to inhibit grain growth in the plane of the film and allows the production of nanoparticles as well as nanocrystalline thin films. For the synthesis of titanium nitride and oxide nanoparticles, sputtering was done in a relatively high pressure (5–100 Pa) of mix gas (O_2, Ar, He, N), after initially evacuating the chamber.

As mentioned previously, a precise determination of the oxygen and nitrogen pressure is required in order to get titanium oxide and nitride with the appropriate stoichiometry. We therefore measure the evolution of the cathode voltage for the different investigated pressures. The results are represented by the curves in Fig. 2. The characteristics do not depend on the temperature for a given pressure.

The curves displayed in Fig. 2 reveal the expected features. The discharge voltage increases when the gas pressure increases up to a threshold. The threshold occurs when the pressure is 50 Pa for N and around 40 Pa for O_2. When it is reached, the cathode voltage shows an abrupt increase due to the full coverage of the target by the oxide or the nitride. After that, the target voltage decreases to a stable value. It is well known that the required titanium stoichiometry, TiO_2, TiN, is obtained after the transition region.

The morphology and particle size distribution in the nanocrystalline samples were studied by standard techniques such as transmission electron microscopy (TEM). The mean particle size was determined in terms of the coherently diffracting crystallographic domain size (d_{XRD}) from X-ray diffraction line broadening (Scherrer technique), after correcting for instrumental broadening.

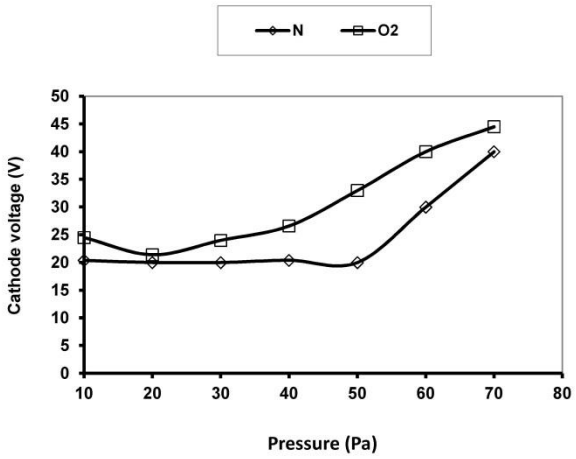

Fig. 2.Cathode voltage versus O_2 and N pressure

Nanocrystalline TiO_2 was produced by vacuum arc sputtering from a target of 99.9% pure metallic Ti. The sputtering gas was a flowing mixture of Argon (95%) and oxygen (5%) at a pressure of 60 Pa. The stainless-steel sample collection plate was maintained at room temperature, at a distance of 200 mm from the target. The sputtering power was 10 kW (40 V, 250A). The as-collected powder was nanocrystalline rutile with $d_{XRD} \approx$ 6 nm and could be heated in air to obtain ultrafine particles of rutile (Fig. 3).

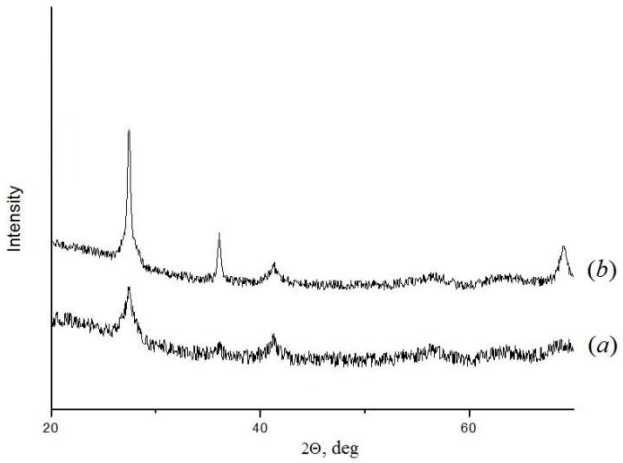

Fig. 3.X-ray diffractograms of a nanocrystalline TiO_2 sample produced vacuum arc sputtering from a target of 99.9% pure metallic Ti. The temperature of the sample holder was 300 K. The XRD from the as-deposited nanocrystalline rutile sample (d_{XRD} = 6 nm) (*a*). This can be converted to nanocrystalline rutile on heating to 350 °C for 4 h (*b*).

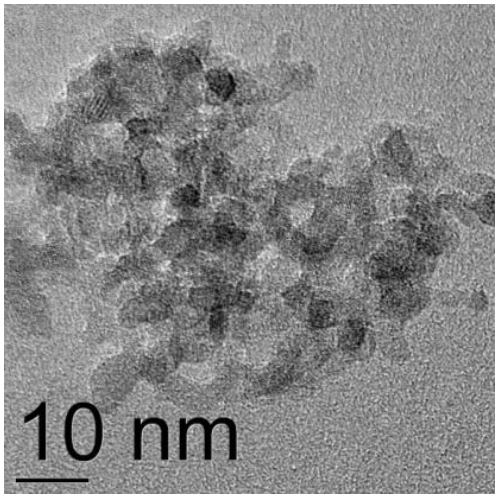

Fig. 4.TEM image of as-sputtered nanoparticles of TiO_2 prepared at a flowing mixture of argon (95%) and oxygen (5%) at a pressure of 60 Pa.

The average particle size, shape, and size distribution of as-collected TiO_2 nanoparticles were investigated using a transmission electron microscope (TEM). TEM micrograph (Fig. 4) of TiO_2 nanoparticles prepared at an oxygen pressure of 60 Pa show an average particle size of 6.7 nm with the standard deviation 0.06. On the other hand, TiO_2 nanoparticles prepared at an oxygen pressure of 70 Pa were observed to have not a reduced average particle size. [15] These results indicate that the feeding of oxygen into the cluster-aggregation chamber controls the size of the nanoparticles, in addition to the phase and structure. As already mentioned, the sputtered Ti atoms lose kinetic energy through successive interatomic collisions with the inert-gas atoms to reach thermal equilibrium and this process leads to an aggregation. On the other hand, the oxidation process upon oxygen feeding into the cluster aggregation chamber utilizes a certain amount of thermal energy from the aggregating sputtering atoms, leading to their early attainment of thermal equilibrium and subsequently results in reduced size of the oxidized nanoparticles. The cluster-deposited TiO_2 nanoparticles have a clean surface and spherical shape as clearly shown in the TEM micrograph of TiO_2 nanoparticles. It is also worth noting that the observed values of the standard deviation 0.06 in these samples reveal the monodispersion of TiO_2

nanoparticles. The cluster-deposition technique has been used to produce a variety of metal and alloy nanoparticles. In a few studies, oxidation of metal clusters such as Fe and Co has been observed by exposing them to an oxygen atmosphere [16, 17]. The oxidation process, however, has been observed to be size-dependent; metal clusters of a few nm in size have oxidized completely, whereas larger nanoparticles exhibited only a partial oxidation [17]. In the present study, the oxidation of Ti clusters, irrespective of their sizes, was controlled precisely by adjusting the partial pressure of oxygen in the gas aggregation region, resulting in the growth of uniform TiO_2 nanoparticles having spherical shape.

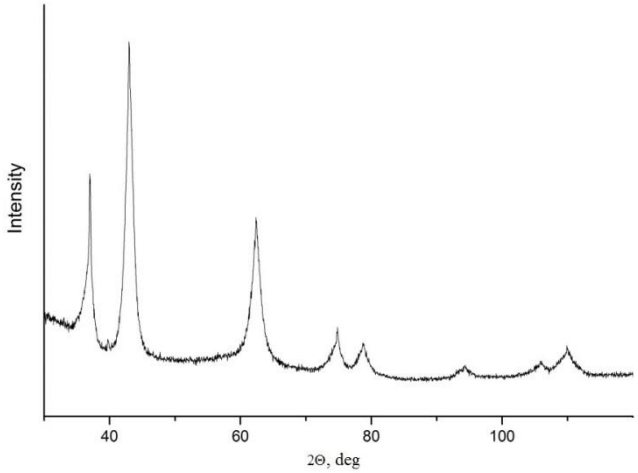

Fig. 5. X-ray diffractograms of a nanocrystalline TiN sample produced vacuum arc sputtering from a target of 99.9% pure metallic Ti.

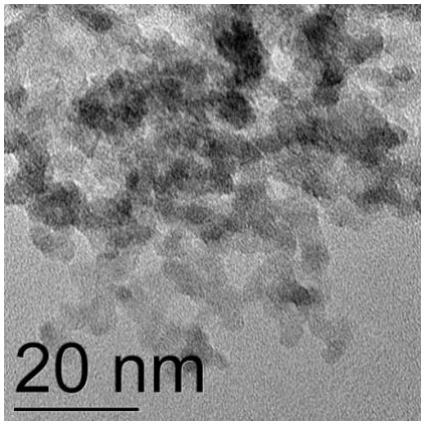

Fig. 6. TEM image of as-sputtered nanoparticles of TiN prepared at a flowing mixture of argon (80%) and nitrogen (20%) at a pressure of 70 Pa.

Nanocrystalline TiN was produced by vacuum arc sputtering from a target of 99.9% pure metallic Ti. The sputtering gas was a flowing mixture of argon (80%) and nitrogen (20%) at a pressure of 70 Pa. The stainless-steel sample collection plate was maintained at room temperature, at a distance of 200 mm from the target. The sputtering power was 4 kW (40 V, 100 A). The specific surface area of the powders exceeds 200 $m^2 g^{-1}$. In X-ray diffraction patterns of high surface area TiN typically broad reflections are observed due to the small particle size (Fig. 5). The peaks can be assigned to cubic TiN. Particle sizes deduced from size broadening of the Bragg reflections come to 8 nm which is close to the particle diameter deduced from TEM (5-12 nm) (Fig. 6) and BET measurements (7 nm). This is, however, within the error limits of the techniques and the assumptions made.

As the specific surface area of the materials is reduced with increasing synthesis temperature, the FWHM is reduced too due to sintering and grain growth within the nanopowders. An important requirement for handling the powders is the stability towards air. In the syntheses described here contact to air must be avoided but the final product is relatively inert towards air. The stability in air was checked for sample by heating the sample to 473 K for 24 h. After the heat treatment the nitrogen content was reduced by approximately 2% from 21.26 to 19.25%. The diffraction pattern was identical to that of the as-prepared sample. A small reduction in nitrogen content is tolerable in terms of bulk composition but indicates passivation layer formation on the outer surface of the particles. The surface chemistry is therefore inevitably changed in air with all implications for catalytic applications. Our high surface area titanium nitride based materials are not suitable for long-term catalytic applications under oxidising conditions but handling in air and regeneration is possible.

It is possible to produce nanoparticles titanium nitride and oxides by physical vapor deposition techniques such as vacuum arc sputtering. Comparatively high gas pressures (40-100 Pa) are used to discourage the formation of continuous thin films. At constant sputtering power, an increase in the atomic mass of the sputtering gas yields larger primary particles on the substrate. This experimental method can be extended easily to produce nanoparticles, irrespective of material systems, from a variety of metal, alloy and ceramic materials with novel functional properties. For titanium nitride based nanoparticles we have demonstrated effective tailoring of surface area and morphology of particles that are only a few nanometers. Our method affords TiN powders with high specific surface areas exceeding 200 m^2 g^{-1}. TEM micrograph of TiO_2 nanoparticles prepared at an oxygen pressure of 60 Pa show an average particle size of 6.7 nm.TiO_2 nanoparticles prepared at an oxygen pressure of 70 Pa were observed to have not a reduced average particle size. It is also necessary to note that the properties of the sputter-deposited samples depend to some extent – rather unfortunately – on the history and surface condition of the target. However, it is relatively simple to use this technique to reduce the average particle size (X-ray domain size) in most materials to about 5 nm through proper choice of substrate temperature, sputtering voltage and gas pressure.

Acknowledgments

This work was supported by the Russian Foundation for Basic Research (projects no. 15-08-02132).

References

1. A.N. Shipway, E. Katz and I. Willner Nanoparticle Arrays on Surfaces for Electronic, Optical, and Sensor Applications. *Chem Phys Chem*. 1 (2000), pp. 18-52.
2. Kamat, P. V. Photophysical, Photochemical and Photocatalytic Aspects of Metal Nanoparticles. *J. Phys. Chem. B*., 106 (2002), pp. 7729-7744.
3. N. P. Melott, C. Durucan, C. G. Pantano, M. Gugliemi Commercial and laboratory prepared titanium dioxide thin films for self-cleaning glasses: Photocatalytic performance and chemical durability *Thin Solid Films*, 502 (2006), pp. 112-120.
4. Arbatti, M.; Shan, X.; Cheng, Z.-Y Ceramic–Polymer Composites with High Dielectric Constant. *Adv. Mater*., 19 (2007), pp. 1369-1372.
5. Li, J.; Seok, S.; Chu, B.; Dogan, F.; Zhang, Q.; Wang, Q. Nanocomposites of Ferroelectric Polymers with TiO2 Nanoparticles Exhibiting Significantly Enhanced Electrical Energy Density. *Adv. Mater*., 21 (2009), pp. 217-221.

6. Li, J.; Claude, J.; Norena-Franco, L. E.; Seok, S.; Wang, Q. Electrical Energy Storage in Ferroelectric Polymer Nanocomposites Containing Surface-Functionalized BaTiO3 Nanoparticles. *Chem. Mater*., 20 (2008), pp. 6304-6306.
7. Harden, E.; Ploumen, S.; Fricke, B.; Miller, T.; Snyder, K. Energy storage devices for future hybrid electric vehicles. *J. Power Sources*., **168** (2007) pp. 2-11.
8. Sarjeant, W. J.; Clelland, I. W.; Price, R. A. Capacitive components for power electronics. *Proc. IEEE*., **89** (2001), pp. 846-855.
9. Simon, P.; Gogotsi, Y. Materials for electrochemical capacitors *Nat. Mater*., **7** (2008), pp. 845-854.
10. Jang HD, Kim SK, Kim SJ. Effect of Particle Size and Phase Composition of Titanium Dioxide Nanoparticles on the Photocatalytic Properties. *J Nanoparticle Res*., 3 (2001), pp. 141-147.
11. T. Sugimoto, X. Zhou, A. Muramatsu. Synthesis of uniform anatase TiO2 nanoparticles by gel–sol method: 3. Formation process and size control. *J of Colloid and Interface Sci*., 259 (2003), pp. 43-52.
12. Feczko, T; Muskotal, A; Gal, L; Szepvolgyi, J; Sebestyen, A; Vonderviszt, F. Synthesis of Ni–Zn ferrite nanoparticles in radiofrequency thermal plasma reactor and their use for purification of histidine-tagged proteins. *J Of Nanoparticle Res*. 10 (2008), pp. 227-232.
13. Takamasa Ishigaki and Ji-Guang Li. Synthesis of functional TiO2-based nanoparticles in radio frequency induction thermal plasma. *Pure Appl. Chem*., 80 (2008), pp. 1971-1979.
14. I.V. Karpov, A.V. Ushakov, L.Yu. Fedorov, A.A. Lepeshev, Method for Producing Nanomaterials in the Plasma of a Low Pressure Pulsed Arc Discharge. *Tech. Phys*., 84 (2014), pp. 559-563.
15. L.Yu. Fedorov, I.V. Karpov, A.V. Ushakov, A.A. Lepeshev, Influence of Pressure and Hydrocarbons on Carbide Formation in the Plasma Synthesis of TiC Nanoparticles. *Inorganic Materials*, 51 (2015), pp. 25-28.
16. Wei, X.-H.; Skomski, R.; Sun, Z.-G.; Sellmyer, D. J. Proteresisin. *J. Appl. Phys.*, 103 (2008), pp. 07D514-1-07D514-4.
17. Qiang, Y.; Antony, J.; Sharma, A.; Nutting, J.; Sikes, D.; Meyer, D. Iron/iron oxide core-shell nanoclusters for biomedical applications. *J. Nanopart. Res*., 8 (2006), pp. 489–496.